Amirkabir Journal of Mechanical Engineering

Amirkabir J. Mech. Eng., 50(4) (2018) 1-3
DOI:

Simulation of Biceps Femoris Muscle Growth Based on Stretch Using a Multiscale Model

S. Javadi[1], A. Jaamialahmadi[1]*, A. Daneshmehr[2], M. Azadvari[3], S. Nekoonam[4]

[1] Department of Mechanical Engineering, Faculty of Engineering, Ferdowsi University of Mashhad, Mashhad, Iran.
[2] School of Mechanical Engineering, University of Tehran, Tehran, Iran.
[3] Department of Physical Medicine and Rehabilitation, Tehran University of Medical Sciences, Tehran, Iran.
[4] Department of Anatomy, School of Medicine, Tehran University of Medical Sciences, Tehran, Iran.

ABSTRACT: The purpose of this research is to investigate the performance of hybrid Darrieus-Savonius wind turbines to achieve a model with high starting moment and suitable performance conditions. Straight-bladed Darrieus wind turbines have high-amplitude fluctuations in moment and, at some angles, this moment is not enough to start the turbine motion. The hybrid turbine is compared with two equivalent models of straight-bladed Darrieus wind turbines. The first model has equal available power and the second model has equal height with the hybrid turbine. Three-dimensional simulation is performed using computational fluid dynamics and solving unsteady Reynolds averaged Navier-Stokes equations with finite volume method, using turbulence model and rotating mesh for rotation of the turbine. According to the results, at the self-starting, the hybrid turbine possesses 22.24% and 17.5% less standard deviation and 69.8% and 56.9% more average moment, respectively, compared to the first and second equivalent turbines. In operational mode, the hybrid turbine at the rotational speed of 30 RPM possesses 16.1% and 27.3% less standard deviation and 19.1% and 1.03% more average moment, respectively. Therefore, the hybrid turbine at the self-starting, as well as at low rotational speeds, possesses more average moment and less fluctuations compared to equivalent Darrieus turbines.

Review History:
Received:
Revised:
Accepted:
Available Online:

Keywords:
Soft tissue growth
Finite element analysis
Hyperelastic
Musculoskeletal
Simulation

1- Introduction

One of the most common musculoskeletal problems is the shortening of hamstring muscles, which can be caused by various factors such as inactivity, chronic neurological diseases or spinal cord injury. This muscle shortening results in the patient's limited range of motion and numerous clinical problems [1]. To treat this disease, the muscle must be stretched in accordance with physiotherapy method to grow. The key question is how much and where are the maximal stretching locations during muscle growth? What is the process of muscle growth over time? The main unit of any muscle tissue is the sarcomere, which consists of two groups of actin and myosin. When the muscle is stretched, it results in a gap between these two groups. In this study, by applying soft tissue growth simulation, in addition to identifying the accurate location of the maximum stretch during growth process, the optimal time duration care of the muscle has been determined.

2- Methods

In order to simulate the growth of muscle, a single cubic element was considered as a skeletal muscle cell. Then the governing equations obtained by combining the continuum mechanics and growth evolution, were coded in an User-defined MATerial (UMAT) subroutine written in FORTRAN. The numerical simulation was performed in Abaqus/implicit software in conjuction with a UMAT for soft tissue behaviour. Finally, a cylinder was considered as the Biceps femoris long head, which is one of the hamstring muscles, and its growth and severe strains were investigated. This simulation is based on a continuum model developed by Zöllner et al. [2]. Hence, the basic equations of this model are shown below.

One of the most important assumptions required for finite growth is decomposition of deformation gradient tensor, Such that

$$\boldsymbol{F} = \boldsymbol{F}_e \boldsymbol{F}_g \quad , \quad \boldsymbol{F}_e = \boldsymbol{F} \boldsymbol{F}_g^{-1} \tag{1}$$

In this simulation, muscle growth is modeled only by increasing or decreasing the sarcomeres along the fibers, therefore, an inelastic deformation gradient proposed for this growth type is as follows [2]

$$\boldsymbol{F}_g = \boldsymbol{I} + [\vartheta - 1]\boldsymbol{n}_0 \otimes \boldsymbol{n}_0 \tag{2}$$

where $\boldsymbol{I}$ is the identity tensor, $\boldsymbol{n}_0$ is the initial material direction, and ϑ is a growth variable that represents the relative serial sarcomere number. In order to extend simple equations for soft tissue, it is assumed that such growth to be homogeneous with isotropic properties. In addition a strain energy function of Neo-Hookean type is adopted, as

*Corresponding author's email: jaami-a@um.ac.ir.com

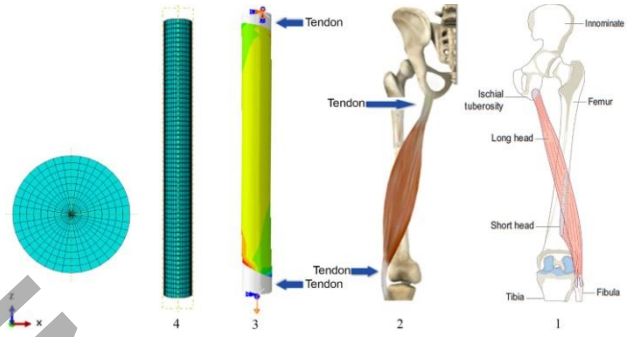

Fig. 1. Finite element model of the assumed cylindrical shape muscle

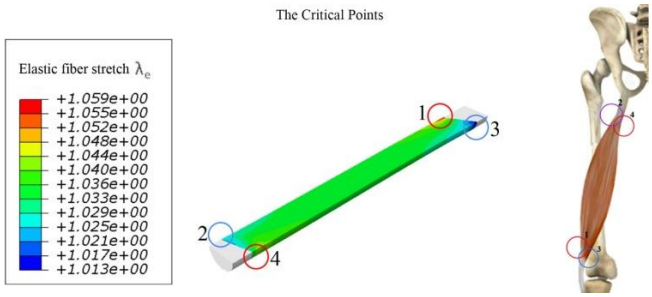

Fig. 3. The longitudinal-section view of the muscle after stretching

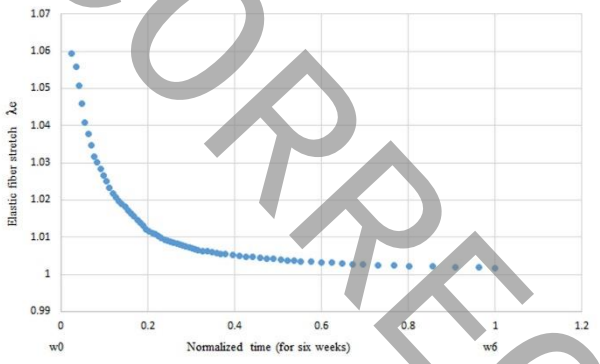

Fig. 2. Dynamic changes in the sarcomere length.

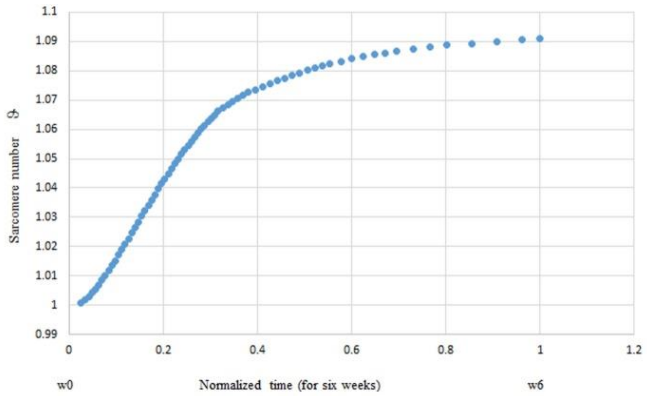

Fig. 4. Dynamic changes in the sarcomere number

$$\psi = \frac{1}{2}c_1 \ln^2(J_e) + \frac{1}{2}c_2\left[\boldsymbol{C}_e : \boldsymbol{I} - 3 - 2\ln(J_e)\right] \quad (3)$$

where c_1 and c_2 are the Lamé constants, $\boldsymbol{C}_e$ is the elastic right Cauchy green tensor, and J_e denotes elastic volume change. The second Piola-Kirchhoff stress tensor $\boldsymbol{S} = 2\partial\psi/\partial\boldsymbol{C}$ and the fourth-order Lagrangian elastic tensor $\boldsymbol{L} = 4\partial^2\psi/\partial\boldsymbol{C}\otimes\partial\boldsymbol{C}$ are derived from the second law of thermodynamics. Furthermore, the Kirchhoff stress $\boldsymbol{\tau} = \boldsymbol{F}\,\boldsymbol{S}\,\boldsymbol{F}^t$ is obtained using a push-forward operation. In this simulation, the evolution Eq. (4) is adopted to calculate the relative serial sarcomere number [2].

$$\dot{\vartheta} = k_g(\vartheta)\,\phi_g(\lambda_e) \quad (4)$$

where $k_g = 1/\tau\left[\vartheta^{\max} - \vartheta/\vartheta^{\max} - 1\right]^{\gamma}$ is the adaptation function and $\phi_g = \langle\lambda_e - \lambda_{\text{crit}}\rangle$ is the adaptation criterion. To solve the nonlinear equations, a finite element computational model was implemented in conjunction with an user subroutine by implicit solver of the Abaqus/standard version 6.13. The relative sarcomere number ϑ is introduced as an internal variable and then its evolution Eq. (4) is solved using a finite-difference approximation method. After determining the amount of new sarcomere ϑ, the growth gradient deformation $\boldsymbol{F}_g$ is calculated from Eq. (2) and the elastic gradient deformation $\boldsymbol{F}_e$ from Eq. (1), too. Finally, the true Cauchy stress $\boldsymbol{\sigma}^{abaqus} = \boldsymbol{\tau}/J$, which the user-defined subroutine in Abaqus/.standard utilizes, is calculated to be applied to the muscle

3- Cylindrical shape muscle model

A cylindrical shape muscle finite element model with a height of 400 mm and a diameter of 20 mm is illustrated in Fig. 1. After a mesh sensitivity procedure, a model with 53487 elements including 38556 linear hexagonal elements of type C3D8 and 14931 linear wedge elements of type C3D6, were generated. For increasing computational efficiency in modeling, because a tendon is much stiffer than muscle tissue, it has been assumed as a rigid member [3]. Biceps femoris's fibers are drawn from distal to proximal in a closed and parallel manner [4]. In this study, this direction is aligned with the stretch axis. The head of the muscle which is attached to the Fibula bone are considered as a movable and the head of the muscle is attached to the ischial tuberosity bone as a fixed boundary condition as well. The boundary conditions and the material parameter are shown in Fig. 1 and Table 1 respectively.

Table. 1. The material parameters

c_1	c_2	τ	γ	ϑ^{max}	λ_{crit}
16 kPa	4 kPa	0.5	2.0	1.1	1.01

4- Results and Discussion

The simulation results of the dynamic changes in sarcomere length for the element with maximum amounts of elastic stretch are plotted in Fig. 2. The graph was drawn in response to a 10% increase in muscle length for a 6-week treatment period. According to this graph, the elastic stretch λ_e decreases from 1.06 to 1 after this time duration. Furthermore, a significant decrease in the elastic fiber stretch during the first two weeks not only does ease the pain but also indicates a high chance of injury at this time.

Fig. 3 shows the cross-sectional view of the muscle after stretching. The red circles represent the maximum stretch location and the blue circles indicate the minimum ones. As can be seen from this figure, these points are the closest points to the myotendinous junction and are located on the inner and outer surfaces of the muscle. De Smet and Best [5] applied magnetic resonance imaging to 15 athletes with hamstring muscle injuries. They showed that all of these injuries furthermore occurred adjacent to myotendinous junction.

Fig. 4 shows the dynamic changes in the number of sarcomeres that were normalized versus to 6 weeks of treatment in response to a 10% increase in muscle length. The growth of sarcomeres was high in the early weeks, leading to a greater flexibility rate than the last weeks.

5- Conclusion

In this study, a biceps femoris long head muscle considered as a cylinder with a model of soft tissue growth was simulated numerically.In this study, a numerical model of soft tissue growth was simulated on a cylinder assumed as a biceps femoris long head muscle. An isotropic behavior and a Neo-Hookean elastic model were used for the muscle material The results showed that the rapid growth of sarcomeres, which lead to severe pain, occurs within the first weeks of treatment duration. Furthermore, the most critical points that tolerate maximum stretch are located in the proximal area on the posterior surface and the distal area on the interior surface of the muscle and on the myotendinous junction. The results of this simulation are in accordance with the results of an investigating of clinical magnetic resonance imaging for 15 athletes with hamstring muscle injuries.

References

[1] W.E. Prentice, Rehabilitation Techniques for Sports Medicine and Athletic Training with Laboratory Manual and ESims Password Card, McGraw-Hill Education, 2005.

[2] A.M. Zöllner, O.J. Abilez, M. Böl, E. Kuhl, Stretching skeletal muscle: chronic muscle lengthening through sarcomerogenesis, PloS one, 7(10) (2012) e45661.

[3] A.M. Zöllner, J.M. Pok, E.J. McWalter, G.E. Gold, E. Kuhl, On high heels and short muscles: a multiscale model for sarcomere loss in the gastrocnemius muscle, Journal of theoretical biology, 365 (2015) 301-310.

[4] N. Palastanga, R. Soames, Anatomy and human movement, structure, and function with pageburst access, 6: anatomy and human movement, Elsevier Health Sciences, 2011.

[5] A.A. De Smet, T.M. Best, MR imaging of the distribution and location of acute hamstring injuries in athletes, American Journal of Roentgenology, 174(2) (2000) 393-399.